Carbonates Evaporites (2014) 29:177–192
DOI 10.1007/s13146-013-0165-2

ORIGINAL ARTICLE

Use of hydrochemistry and environmental isotopes for assessment of groundwater resources in the intermediate aquifer of the Sfax basin (Southern Tunisia)

Zohra Hchaichi · Kamel Abid · Kamel Zouari

Accepted: 3 July 2013 / Published online: 4 August 2013

Abstract Groundwaters from the intermediate aquifer of Sfax basin have been investigated using chemical tracers and environmental isotopes to reveal the hydrogeological features of this system and characterize the dynamics of groundwater salinization in this sector. The origin of salinity in the studied aquifer was investigated based on the chemical analyses of 30 groundwater samples. Groundwater is characterized by Na–Cl and Na–SO_4 water types. The saturation indices for calcite and gypsum, and binary diagrams of different ions showed that the main hydrogeochemical processes were the dissolution of carbonates (mainly calcite scattered through the reservoir rocks), the dissolution of evaporites (halite, gypsum and anhydrite) and the cation exchange processes. The isotopic composition investigation allowed the definition of two groups. The first group is represented by groundwater with the highest oxygen-18 content ($\delta^{18}O$ ranges between −5.36 and −4.22 ‰, and $\delta^{2}H$ ranges between −39.2 and −36 ‰). The high $\delta^{18}O$ values in this group can be attributed to the evaporation effect. The second group includes the most depleted waters ($\delta^{18}O$ varies between −6.84 and −5.79 ‰, and $\delta^{2}H$ varies between −42.4 and −36.5 ‰). The combined analyses of stable isotopes and major ions (Cl^{-}) showed that mixing between old and recent water and evaporation were the main processes explaining the variation of salinity of the intermediate aquifer of the Sfax basin.

Keywords Tunisia · Hydrogeochemical · Dissolution · Cation exchange · Evaporation

Z. Hchaichi (✉) · K. Abid · K. Zouari
École Nationale d'Ingénieurs de Sfax, BP 1173, 3038 Sfax, Tunisia
e-mail: zohraelhcheichi@yahoo.fr

Introduction

Carbon isotopes of DIC and stable isotopes of water have long been used as groundwater tracers (Fontes and Garnier 1979; Plummer et al. 1976; Aravena et al. 1995; Clark and Fritz 1997). 14 C is the most reliable chronometer of moderately old groundwater (5 ± 30 kyr), although corrections should take into account water–rock interactions. Stable isotopes have been used to identify possible recharge areas and mixing within aquifer systems. However, in regional studies, interpretations of stable isotopes data are getting more complex because their input functions vary with a number of different factors including elevation, precipitation amount, continentality and long-term climate change (Clark and Fritz 1997; Dansgaard 1964; Rahoui and Koshel 1980).

The salinity of water resources has been intensively studied during the past decades, particularly in coastal aquifers, stimulated by both scientific interest and social need (Custodio 1987; Richter and Kreitler 1993; Fedrigoni et al. 2001; Vengosh 2003; Vengosh et al. 2005, 2007; Petalas and Diamantis 1999).

Sustainable management of available groundwater reserves is almost impossible without adequate knowledge of the spatial distribution of groundwater salinity and the processes involved in the observed spatiotemporal variations. As present-day distribution of groundwater salinity in aquifers still reflects former hydrological conditions, it is often unclear whether the current situation is the result of long-term (geological) processes or recent (anthropogenic) changes (Edmunds et al. 2003; Vengosh et al. 2005; Bennetts et al. 2006; Rahoui and Koshel 1980). Understanding the processes and factors that control the evolution of saline water in aquifers over the years is an academic challenge and has important practical implications for water resource evaluation and management.

In Tunisia, particularly in the south of the country, groundwater is the main water resource and is used by agriculture (80 %), industry (10 %) and domestically (5–10 %). The Sfax region, located on the east coast of the country, has an underground water system composed of a deep confined aquifer and shallow aquifer that are delimited by their respective catchment areas. Recently, water management authorities have been facing problems associated with declining water quality and increasing demand for water through population and economic growth and improved standards of living that accompany such changes.

During semi-arid climatic conditions, water resources of the Sfax area seem to be very limited compared to the considerable demand of the agricultural and industrial sectors. In addition, the groundwater of the shallow aquifer is characterized by a reduced water volume and high water mineralization. This aquifer is exposed to overexploitation and seawater intrusions (Plummer et al. 1976; Trabelsi et al. 2008).

The greatest part of water needs in the Sfax region is supplied by the Miocene deep aquifer. Indeed, up to 10 million cubic metres of water were annually pumped from this aquifer during the period from 1978 to 1986. Between 1987 and 2000, the annual amount of extracted water has increased to some 26 million cubic metres (McLean et al. 2000).

The hydrogeological study (El Batti and Andrieux 1977; Beni Akhy 1994; Fedrigoni et al. 2001; Trabelsi et al. 2005) of this region showed that the Sfax plain is composed of two main aquifers: a shallow aquifer (Plio–Quaternary) overlying a deep aquifer (Miocene).However, recent studies have proved the existence of an intermediate aquifer in the detrital Mio–Pliocene deposits.

In this study, the intermediate aquifer system of the Sfax region has been the subject of a geochemical investigation including analyses of major elements, stable isotopes (^{18}O, ^{2}H, ^{13}C) and radio-carbon dating. The objectives were to (1) quantify the recharge of the aquifer, (2) specify the

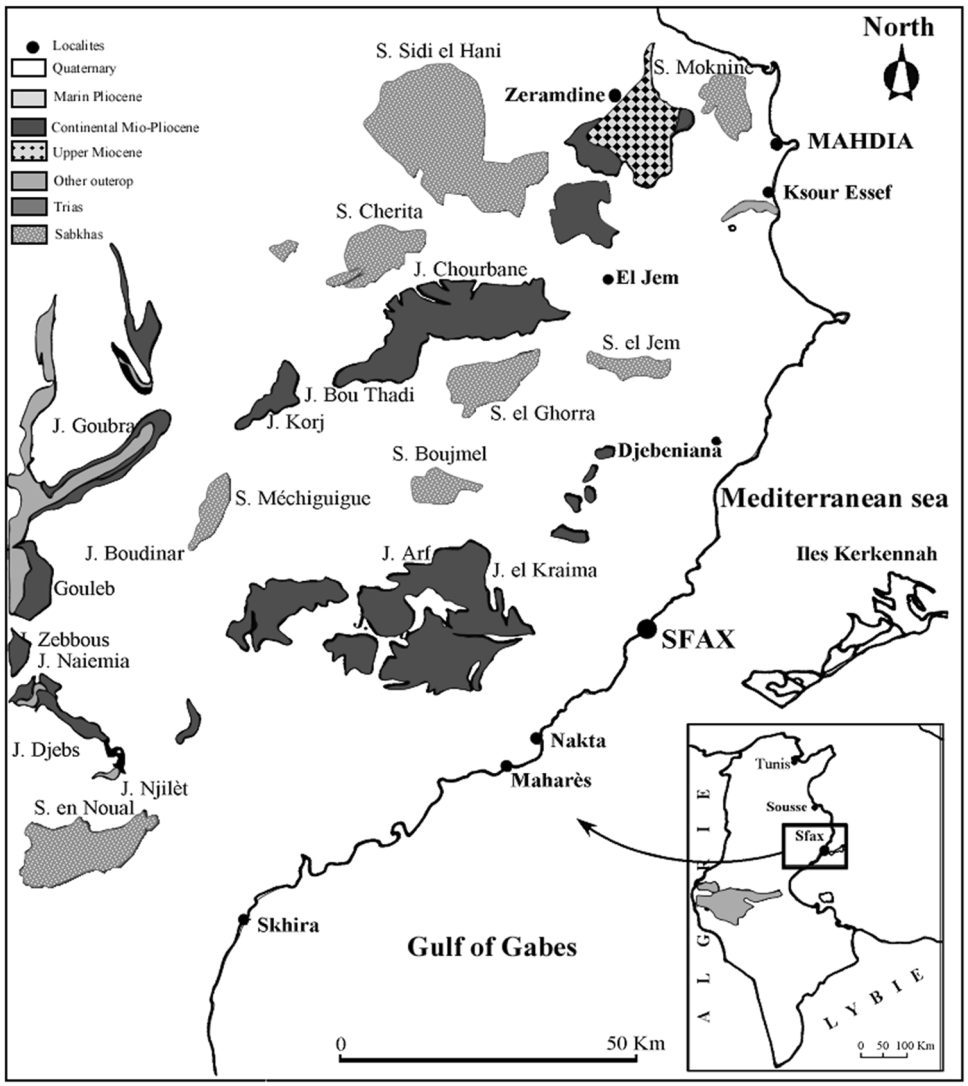

Fig. 1 Geological map of the studied area

origin of the mineralization of the groundwater and (3) estimate the average residence time of groundwater.

Study area

The Sfax region, located in the east coast of Tunisia, is the second major urban area after Tunis (1.2 M of inhabitants). It is a large economic pole (first oil producer, first fishing port, second industrial pole, oil and gas producer) whose various activities require availability of significant water resources. The water demand increased from 48 Mm^3/year in 1995 to 84 Mm^3/year in 2006 (Belgacem et al. 2010).

The Sfax basin is bordered to the east by the Mediterranean Sea, the N–S axis mountain chain to the west, the Korj Bou Thadi, Chorbane, Zeramdine and Djemmel Hills to the north and Mezzouna Mountain in the south (Fig. 1). Four Sebkhas (salt plain) can be observed in the west. The study area is characterized by an arid climate where precipitations are rare (average annual precipitation around 250 mm). The temperature is relatively high with an average of 19 °C/year.

Geology and hydrogeology

The geology of the area was described by Castany (1953), Burollet (1956), Zebidi (1989). The Sahel of Sfax area is characterized by a monotonous topography with little accented bulges, separated by wide basins occupied by Sebkhas.

The geology of the study area is dominated by outcrops of the Mio–Pliocene and the Quaternary deposits. More or less affected by the major tectonic phases Ben Akacha (2001); the study area presents anticlines at large radii of curvature with altitude less than 200 m (Belgacem et al. 2010).

The lithology includes the Souar Formation, considered to be of Eocene age and composed of sediments deposited in a marine environment Bouaziz (1994). The Oligocene sediments are composed of a lower marine unit and an upper continental sandy one.

The Miocene presents an important thickness with alternating clay, sand and sandstone units. It is divided into three units (Tayech 1984), including the Ain Ghrab Formation (Burdigalian) that mainly consists of limestone interlayered in the lower part with gypsum, the Oum Douil

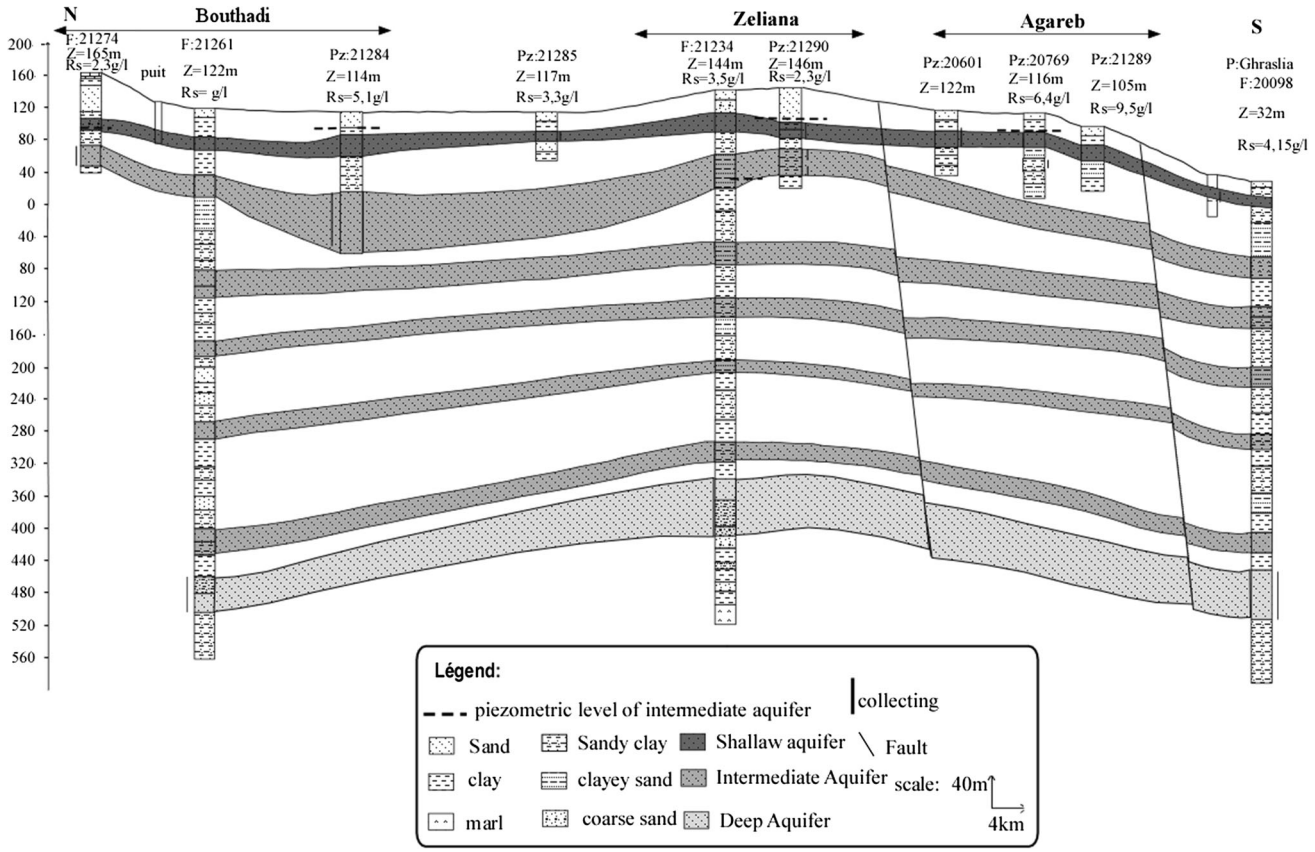

Fig. 2 Hydrogeological cross section in the Sfax basin

Formation (Langian to Tortonian) consisting of a variable proportion of silt and clay and the Segui Formation (Messinian) composed of continental sand, silt, and clay alternations.

The Pliocene deposits discordantly overlie the older Formations and consist of marl units. The Pleistocene is divided into two units: the lower one, characterized by calcareous sand, and the upper one of silt and gypsum. The Holocene is characterized by granular materials of various origins overlying clayey formations.

The Upper Miocene, Pliocene and Quaternary sand and silty clay deposits constitute the reservoir of the superficial aquifers of the region. These deposits present several productive layers separated by semi-permeable layers.

As shown in the hydrostratigraphic N–S cross section, three aquifers are present in the basin of Sfax.

The shallowest aquifer, which is an unconfined superficial unit, is located in the Quaternary and Mio–Pliocene layer system formed by sand and silty clay which are separated by sandy-clays (Hajjem 1980; Maliki 2000). Its thickness varies from 8 to 60 m, with an average of 30 m. The base of the reservoir is formed by a clayey–sandy unit of continental origin, characterized by alternations of unrefined sand, and conglomerates with passages of red sandy marls and clays.

Generally, these water-bearing formations have an alluvium character and possess a lenticular geometry, a limited horizontal area and an irregular vertical continuity. Based on pumping tests, the transmissivity was estimated to 1.5×10^{-3} m^2/s (Maliki 2000; Rozanski et al. 1993).

The flow of water from this aquifer is multidirectional. The aquifer is recharged by direct infiltration and its highest points located in the north and the west of the basin. The discharge areas are found on the Mediterranean shoreline and the Sebkhas. This aquifer system has very large reserves at the regional level, easily accessible but highly vulnerable to pollution and overexploitation. The salinity rises from 0.3 to 23 g/l where seawater intrusion affects the water quality.

This aquifer is also believed to be overexploited, especially near the coast. In addition, the quality of the water that it contains has become degraded owing to increased

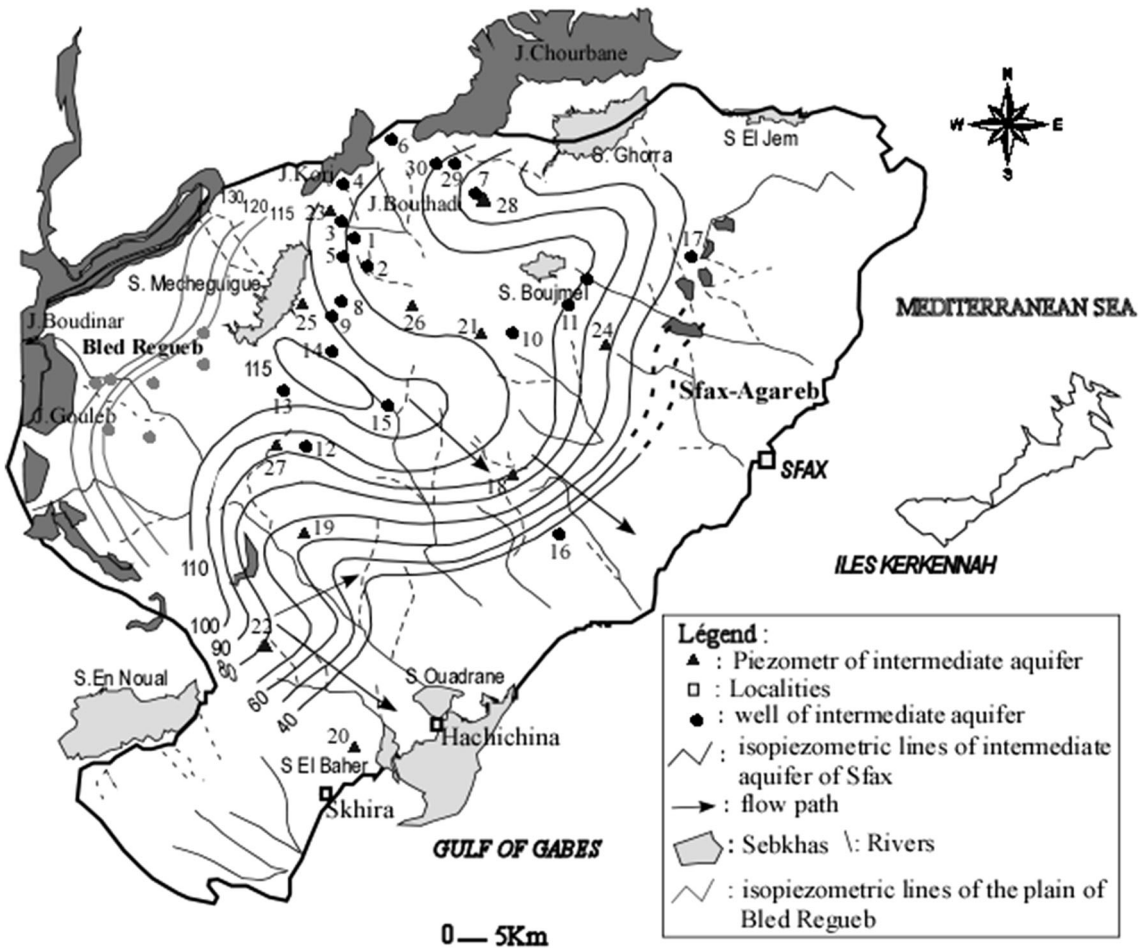

Fig. 3 Piezometric map of intermediate aquifer of the Sfax aquifer in 2008

exploitation through the construction of new pumping wells, the intrusion of seawater and the infiltration of water that has been used to irrigate crops. Until recently, the lack of any synthesis, interpretation and archiving of data concerning this aquifer had led to the lack of its accurate description. This, in turn, led to the region's water resources being undervalued, and hence to difficulties in establishing a suitable management plan.

The intermediate aquifer, which is situated between the shallow and deep aquifer, the main objective of this study, was identified in recent wells at a depth of 80–300 m. It is constituted of 150–300 m of sand and sandy clay deposits attributed to Pliocene and Quaternary. This aquifer increases in thickness from north to south (Fig. 2). It constitutes a multilayered aquifer system differentiated into several units of detrital sediments separated by clay-rich strata, giving rise to heterogeneity in this aquifer. Some thin but relatively permeable layers may be important in controlling the hydraulic continuity. Transmissivities obtained from pumping tests range from 1×10^{-4} to 4.32×10^{-3} m ^{2}/s. The renewable water resources of this intermediate aquifer were estimated at 11.6 Mm^3/year.

The piezometric map of the Sfax intermediate aquifer (Fig. 3) was made with reference to 30 wells and piezometers. This map shows that the main groundwater flow direction is NW–SE from the recharge areas constituted bythe N–S axis mountain chain in the west, and the Korj Bouthadi, Chorbane, Zeramdine and Djemmel hills in the north of the basin towards the Mediterranean Sea, which form the natural discharge area.

The Miocene deposits make up the deepest aquifer. It constitutes the principal aquifer of the region. It is formed of sand and sandstones interbedded with clay varying in thickness, with a maximum thickness occurring in the central part of the basin. This aquifer is located at depths between 200 and 700 m; its average thickness is 250 m and covers an area of about 15,000 km^2. The calculated transmissivity ranges between 0.12×10^{-3} and 22.5×10^{-3} m^2/s. The deep aquifer is an important water source in the study area because of its relatively significant thickness and its water quality that is typically better than in the overlying aquifers.

Groundwater flow directions of this aquifer are generally NE, from the heights of the north–south axis to the SW (Skhira

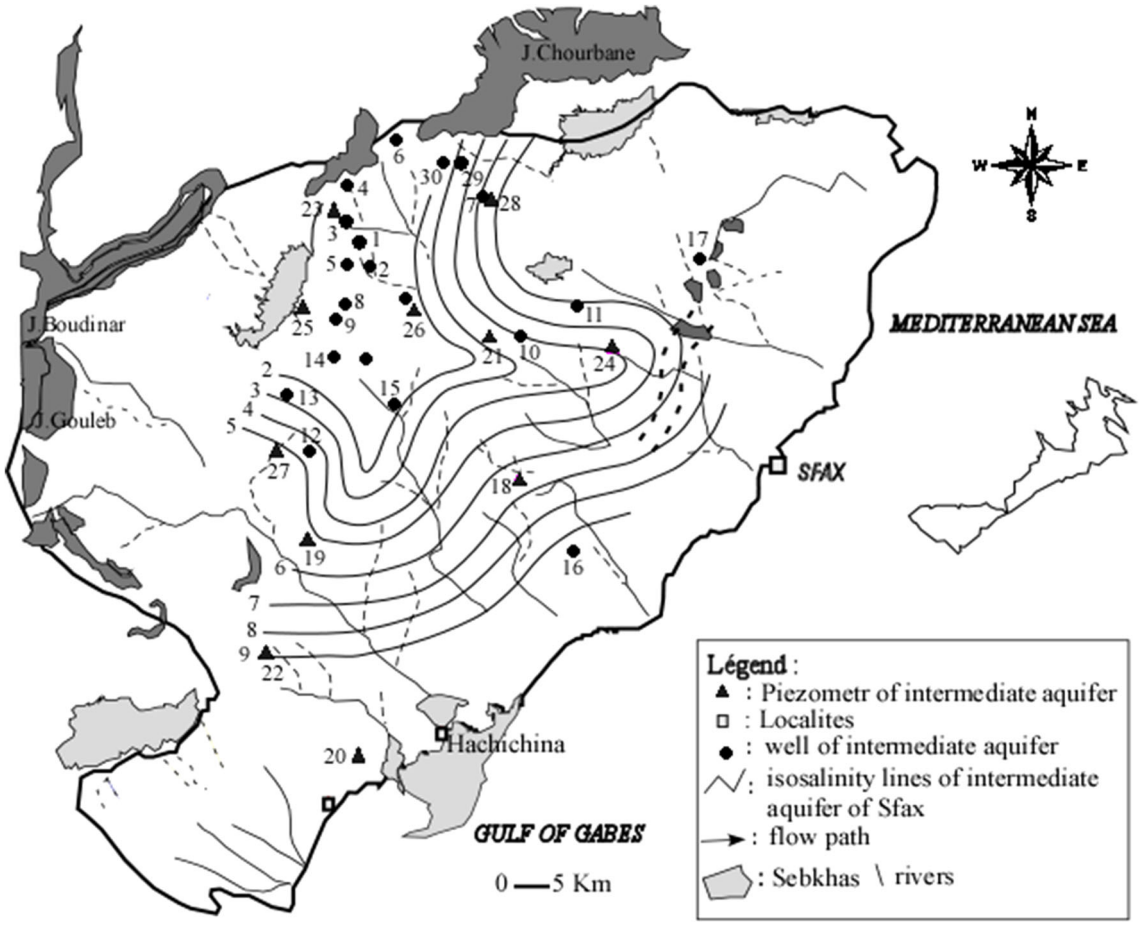

Fig. 4 Spatial distribution of the TDS content (g l^{-1}) of the groundwater in the intermediate aquifer of Sfax

Table 1 Isotopic and geochemical data for the intermediate aquifer of the Sfax basin

Well no	Names	Cl^- (mg/l)	SO_4^{2-} (mg/l)	CO_3^{2-} (mg/l)	HCO_3^- (mg/l)	NO_3^- (mg/l)	Na^+ (mg/l)	K^+ (mg/l)	Mg^{2+} (mg/l)	Ca^{2+} (mg/l)
1	Tarek fourati 2	492.1	2,392.6	0	170.8	82.05	812.3	21.3	173.6	385.3
2	Zied fourati 1	324.2	2,722.85	0	164.7	89.15	754	0	188.95	439.15
3	Amna fourati 2	292.05	2,459	0	195.2	51.1	734.5	0	147.5	358.5
4	Kamel kchaw	485.35	2,225.9	0	176.9	244.8	830.6	0	168.65	332.75
5	Amna fourati 1	1,483.05	1,445.25	12	164.7	34.3	907.15	0	156.6	329.75
6	OTD essalama	416.7	2,418.05	0	292.8	77.25	846	0	153.85	264.85
7	Hafed jerraya 2	1,869.4	1,767.25	0	146.4	58.4	1,206.3	0	249.8	376
8	N ben abd Jelil	251.7	1,153.68	0	195.2	28.73	341.73	10.35	78.35	249.28
9	Chedly kchaw	352.84	2,048.48	0	122	20.52	542.44	0	144.12	309.52
10	O. Mezghanni	260.73	1,081.25	0	219.6	55.48	428.23	0	61.08	157.45
11	Jamil Triki	493.32	1,982.28	0	164.7	38.28	755.16	0	155.6	369.8
12	Ali Chouket	1,387.45	1,856.2	0	134.2	32.55	922.75	0	171.6	380.6
13	Khaled Ellouze	445.2	1,601.04	0	146.4	28.68	574.4	0	94	268.72
14	Bechir Jerraya	357.4	1,931.6	12	103.7	46.16	613.44	0	102.28	272.76
15	Boujlida	335.96	1,636	0	213.5	19.12	659.64	0	103.4	203.48
16	M Gouiaa	2,138.8	2,501.2	0	128.1	2.7	1,275	0	224.1	670.9
17	Hafed gargouri	257.45	1,350.35	0	298.9	11.3	601.63	0	66.53	145.78
18	pz O mabrouk	1,397.8	2,488.85	30	134.20	36.97	1,169.10	0.00	173.82	779.71
19	pz el Gandoul	1,154.05	2,339.85	12	109.80	36.79	816.82	0.00	134.79	684.79
20	pz Siap Skhira	1,256.9	2,907.55	18	79.30	0	935.75	0.00	159.30	886.41
21	pz Zeliana 3	207.025	831.65	24	109.80	28.016	320.45	0.00	89.62	145.41
22	pz Mghadia 2	2,008.9	4,004.3	0	115.90	0	1,215.60	0.00	338.48	1,466.12
23	pz Ennajeh	2,457.8	5,424.4	24	134.20	0	1,833.64	0.00	369.57	1,269.57
24	pz Bir Mellouli	323.52	2,438.6	18	128.10	22.78	383.05	89.38	201.89	626.24
25	pz Sidi Daher	193.2	2,093.32	12	85.40	32.97	816.02	111.96	57.06	175.38
26	pz Hj.Gacem3	206.1	902.3	24	134.20	58.04	364.81	0.00	72.69	178.62
27	pz El kahia	78.16	698	12	183.00	17.49	210.55	0.00	74.95	113.55
28	Hafed Jerraya1	2,591.1	3,404.3	6	140.30	0	1,663.05	0.00	332.66	906.90
29	Abd Aziz Drira	395.4	1,510.625	12	109.80	14.25	745.96	0.00	62.49	209.95
30	CJFR	307.02	921.74	30	207.40	80.61	375.63	0.00	64.42	180.85

Table 1 continued

Well no	Names	TDS (g/l)	T °C	EC (ms/cm)	pH	$\delta^{18}O$ (‰ VSMOW)	$\delta^{2}H$ (‰ VSMOW)	^{14}C (pcm)	Depth (m)
1	Tarek fourati 2	4.83	23.8	5.43	7.64	−6.63	−42.4	23.3	95.3
2	Zied fourati 1	4.99	24.2	5.36	7.44	−6.08	−39.5		90
3	Amna fourati 2	4.5	22.5	5.08	7.4	−6.45	−40.2		80
4	Kamel kchaw	4.81	19.5	5.63	7.4	−5.79	−36.5	44	129
5	Amna fourati 1	4.93	25	5.74	7.4	−6.84	−42.4		85
6	OTD essalama	4.46	22.4	5.2	7.22	−6.42	−39.1	40.6	116
7	Hafed jerraya 2	5.91	23.9	7.95	7.5	−5.15	−34.8	12.2	180
8	N ben abd Jelil	2.52	24.5	3.12	7.22	−6.22	−40.9	46.4	94
9	Chedly kchaw	3.77	24.8	4.3	7.11	−6.43	−40.9	14.4	100
10	O. Mezghanni	2.31	24.9	3.03	8.66	−6.62	−37.2	26.7	114
11	Jamil Triki	4.16	24.5	5	8.64	−6.22	−40.9	22.1	115
12	Ali Chouket	5.01	24.5	6.57	6.98	−6.68	−43.6	20.4	103
13	Khaled Ellouze	3.4	24	4.21	7.01	−6.57	−37.7	22.2	150
14	Bechir Jerraya	3.54	23	4.29	6.93	−5.36	−39.2		85
15	Boujlida	3.41	23.8	4.23	6.9	−6.4	−37.3		120
16	M Gouiaa	6.95	23.5	8.98	6.96	−6.2	−36.5		114
17	Hafed gargouri	3	25			−6.66	−41.6		150
18	pz O mabrouk	6.4	24.4	8.5	7.53	−5.25	−35.7		100
19	pz el Gandoul	5.48	27.7	6.36	7.6	−5.34	−37.8		72
20	pz Siap Skhira	6.28	22.8	7.11	7.51				100
21	pz Zeliana 3	2.9	24.2	3.8	7.65	−4.53	−31.1	38.8	150
22	pz Mghadia 2	9.55	24.5	11.4	7.8	−4.22	−36		85
23	pz Ennajeh	11.71	24.5	13	7.64	−4.42	−33.8		100
24	pz Bir Mellouli	4.2	23.4	5.27	7.72	−4.87	−33.3		82
25	pz Sidi Daher	3.86	23.9	4.16	7.8	−5.03	−35.1	22	100
26	pz Hj.Gacem3	1.93	25	3.06	7.4	−4.97	−35.8	49.2	85
27	pz El kahia	1.42	26.6	2.06	7.75	−5.3	−32.3	56.7	75
28	Hafed Jerraya1	9.79	23.4	12.51	7.45	−4.87	−33.3		160
29	Abd Aziz Drira	3.64	23.1	3.92	7.52	−4.96	−30.5		108
30	CJFR	2.27	22	3.3	7.4	−4.9	−30	47.9	120

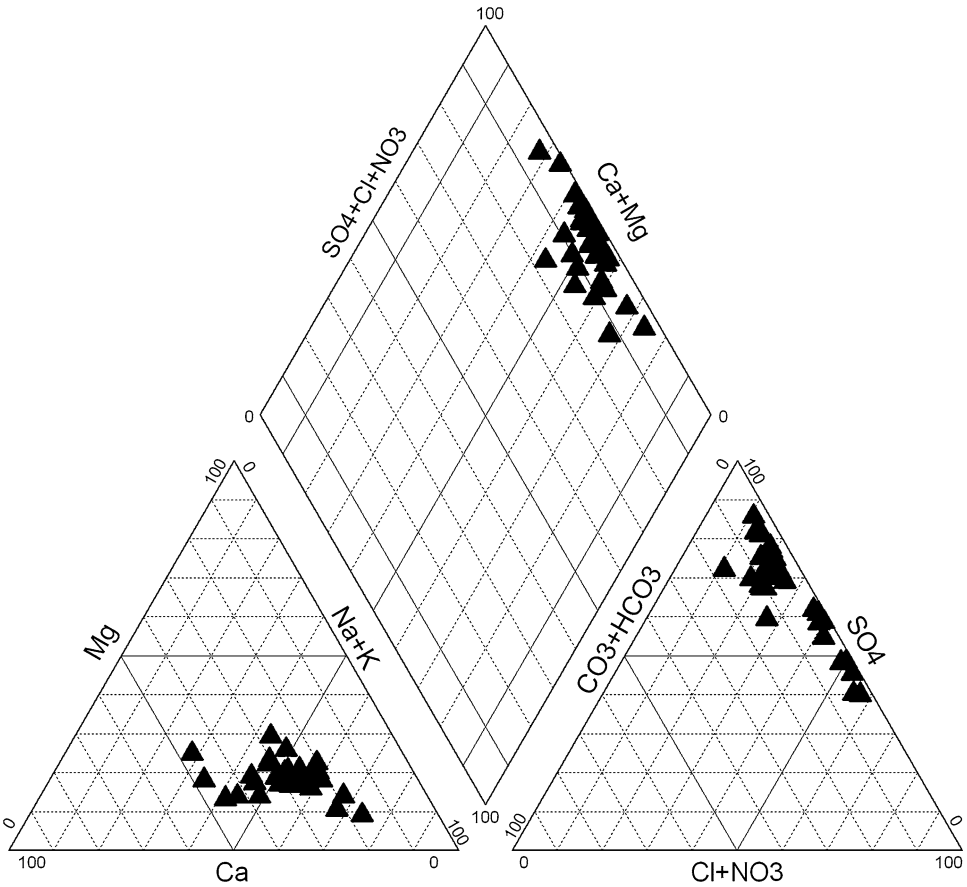

Fig. 5 Piper diagram of the groundwater samples

region); the salinity varies from 3 to 10 g/l. However, in most of the basin, the salinity is less than 4.5 g/l. In the south, around Skhira, however, the salinity is closer to 9 g/l.

Despite the increasing exploitation, the piezometric monitoring from 1987 to 2011 showed only an average annual decrease of 0.3 m. Indeed, volumes rose from 18 Mm^3 in 1988 to about 25 Mm^3 in 2008. Along the coast this aquifer is artesian, whereas in the centre of the basin it is captive. Its exploitation is meant for various purposes such as agricultural (31 %), industrial (55 %) and domestic uses (14 %).

Analysis of tritium, an isotope of hydrogen, revealed the absence of an actual refill of the aquifer. This was confirmed using measurements of carbon isotopes, which suggest that the water in the deep aquifer has been present between 14,000 and 38,000 years without being added to and can be regarded as "fossil" water.

Method and sampling analyses

About 30 water samples were collected during the sampling campaign from June 2007 to August 2007, from piezometers and wells with depths varying from 80 to 200 m, in different parts of the basin (Fig. 4), and were analysed for their chemical and isotopic (^{18}O, ^{2}H) compositions. These different depths were chosen to highlight the relationship between the intermediate and the shallow aquifers.

Groundwater was also sampled for 14 C analyses. The temperature, pH and electrical conductivity (EC) of the water samples were in situ measured. Chemical analysis of the water samples were carried out in the "Laboratory of Radio-Analyses and Environment" of the School of Engineers of Sfax, Tunisia. Major cations (Ca, Mg, Na, and K) and anions (Cl, SO_4 and NO_3) were analysed by ion chromatography (detailed technique).

The isotope analyses were carried out in the laboratory of the International Atomic Energy Agency, Vienna and in the laboratory of Radio Analyses and Environment in the Engineering School of Sfax (LRAE), Tunisia. Stable isotopes were analysed by mass spectrometer and radioactive isotopes by liquid scintillation counting (LSC).

Results and discussions

Chemistry of groundwater

The pH, temperature, EC, TDS and major ion concentrations for water samples from the studied aquifer are

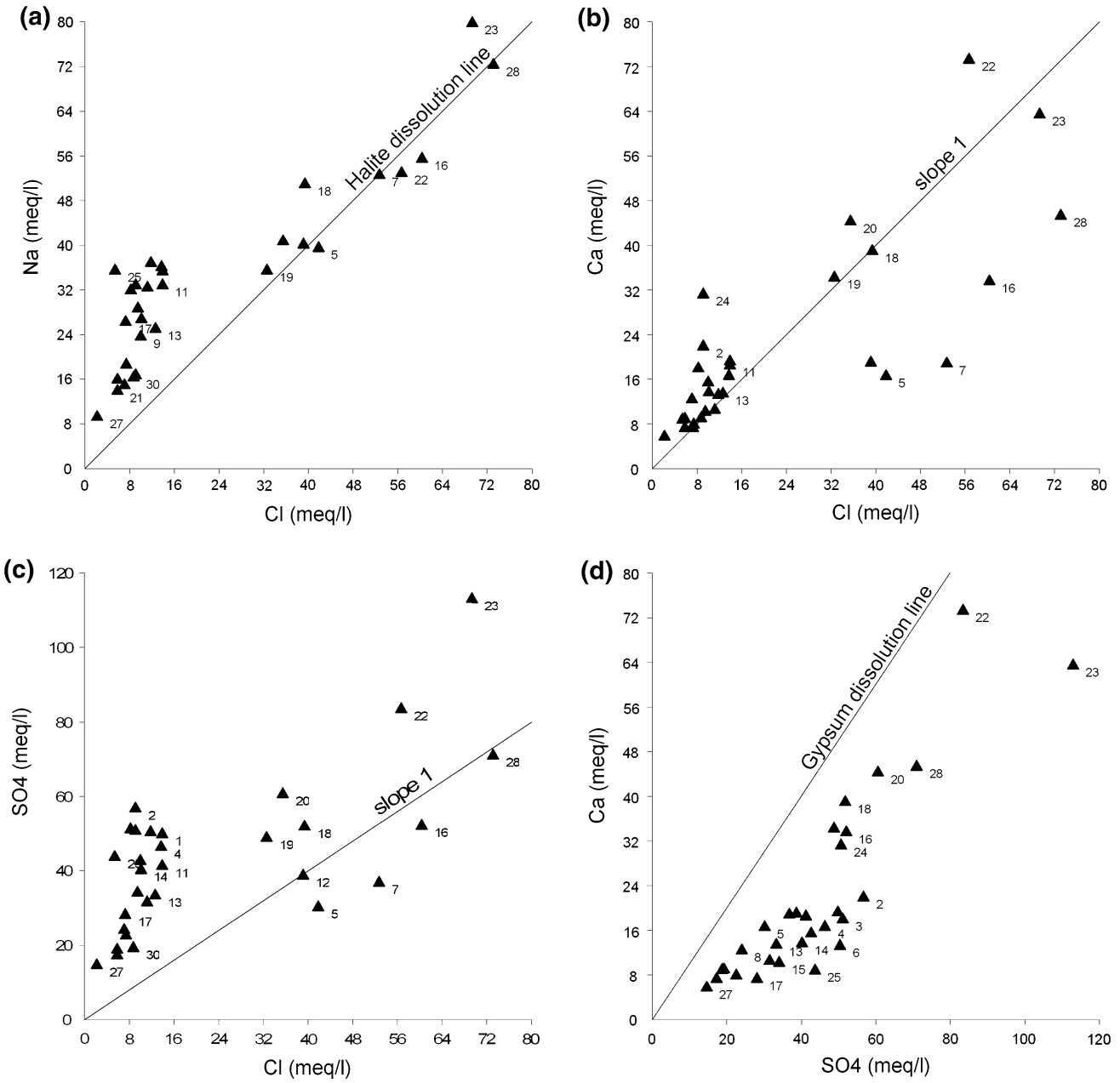

Fig. 6 Relationships between major elements in the analysed groundwater samples: Na–Cl (**a**), Ca/Cl (**b**), SO_4/Cl (**c**) and Ca/SO_4 (**d**)

presented in Table 1. All analyses of water samples present charge balance errors <5 %. Samples collected from the intermediate aquifer of Sfax basin are characterized by high electrical conductivity varying from 1,140 to 13,000 µS cm^{-1}. Temperature in the groundwater samples ranges from 19.5 to 27.7 °C.

The salinity (total dissolved solid contents) of the Mio–Pliocene aquifer is very heterogeneous, varying between 2 and 9 g/l (Fig. 4). The behaviours of ion concentrations, in general, are similar to the EC and the TDS values of the groundwater. Higher values of theses parameters characterize the wells located in the southern part of the basin (discharge zone), especially in the Skhira region, suggesting both the insufficiency of recharge in this part and the relatively long-term water–rock interaction and the evaporation effect, along with anthropogenic activities (agricultural and industrial). Generally, TDS increases from highly elevated areas towards the Mediterranean Sea which constitutes the discharge area. The increase in salinity seems to be related to hydrodynamic degradation as suggested by similarities in piezometry and salinity maps (Figs. 3, 4).The spatial distribution partially conforms to the main groundwater flow direction, indicating that the groundwater salinity is in some way controlled by the

residence time in the aquifer. Relatively low TDS values characterize wells located near the drainage network and reveal the dilution of groundwater by the water from linear recharge. However, high values of TDS depend on the direction of the groundwater flow.

A preliminary characterization, carried out using the Piper triangular diagram (Piper 1944), is shown in Fig. 5. This diagram is used to obtain a preliminary geochemical characterization through the identification of different types of groundwater. It shows that most groundwater samples are characterized by two types of systems: Na–Cl and Ca–SO_4. Most analysed groundwater samples are rich in SO_4^{2-}. A slight Cl^- increase has been observed in the extreme southern part of the studied aquifer. Furthermore, hydrochemical investigations show occurrence of geochemical processes, such as a simple dissolution and cation exchange (Petalas and Diamantis 1999; Petalas et al. 2009).

Geochemical characteristics and origin of mineralization

To highlight different mechanisms that contribute to groundwater mineralization, bivariate diagrams of major elements and chloride were investigated (Fig. 6). The Na^+–Cl^- relationship has often been used to identify mechanisms responsible for the origin of water salinity in arid and semi-arid regions (Magaritz et al. 1981; Dixon and Chiswell 1992; Guendouz et al. 2003).

The relationship between Na^+ and Cl^- shows (Fig. 6a) that the majority of saline water cluster lies along the halite dissolution line. This dissolution is verified through: firstly, the general increasing trend in the Na and Cl concentrations along the groundwater flow direction; secondly, the inverse parabolic correlation between (Na + Cl) and the negative saturation indexes, which indicates an undersaturation state of groundwater with respect to the halite (Fig. 8f).

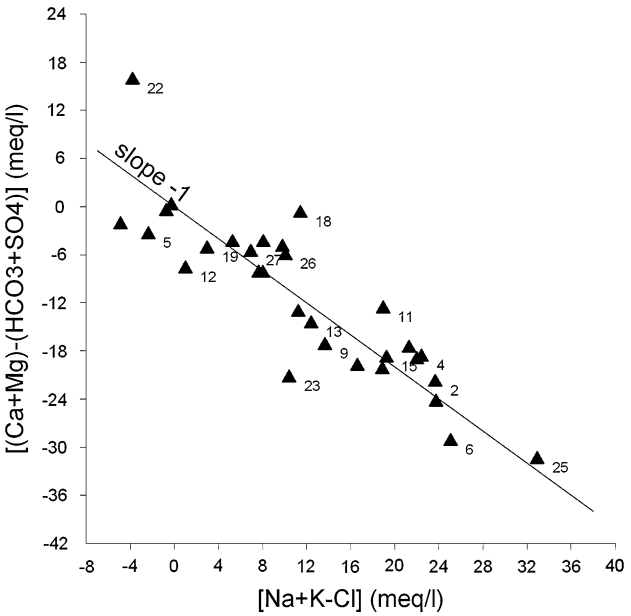

Fig. 7 Plot of [(Ca + Mg)–(HCO_3 + SO_4)] versus [Na + K–Cl]

For some samples (pz sidi daher, OTD essalama, Kamel kchaw, tarek fourati, Amna fourati, jamil triki, abd aziz drira, zied fourati, boujlida, hafed gargouri, chedly kchaw, khaled ellouze,bechir jerraya), a relative excess of Na^+ with respect to Cl^- is observed (Fig. 6a). This Na excess is probably due to the cation exchange process (Abid et al. 2009, 2010; Trabelsi et al. 2008) as shown in Fig. 7 where a decrease of Ca + Mg is compensated by a drop of Na + K (Garcia et al. 2001).

The high values of SO_4^{2-} relative to Cl^- observed in Fig. 6c indicate that the dissolution of gypsum contributes to groundwater salinization.Moreover, calcium and sulphate reveal a positive correlation with chloride (Fig. 6d, c) suggesting that any increase in SO_4^{2-}, Ca^{2+} and Cl^- (Fig. 6b) applies to most of the aquifer and is probably from a uniform source of gypsum/anhydrite with some halite within water-bearing formations. However, the depletion in Ca^{2+} contents relative to SO_4^{2-} concentrations as shown in Fig. 6d is probably due to cation exchange reactions which absorb Ca^{2+} on the clay fraction as Na^+ is released.

The positive correlation between Ca and SO_4 (Fig. 6d) suggests that dissolution of anhydrite and/or gypsum is another major salinization process. Indeed, saturation indexes show that some samples are undersaturated with respect to gypsum and anhydrite.

These saturation indexes, which vary in inverse proportion to the sum of Ca and SO_4, (Fig. 8d, e), were chosen to confirm that the geochemical condition (for the referred samples) was dominated by the dissolution of the anhydrite and gypsum minerals.

To study this assumption, saturation state of the waters with respect to gypsum, dolomite, calcite and halite were performed using WATEQ-F programme (Rozanski et al. 1993). Saturation conditions can be expressed as the ratio between IAP (ion activity product) and K (solubility product), as the saturation state $\Omega = \text{IAP/K}$. Thus there is equilibrium for $\Omega = 1$, oversaturation when $\Omega > 1$ and undersaturation when $\Omega < 1$. For larger deviations from equilibrium, a logarithmic scale can be normally used like the saturation index, SI. However, equilibrium is not reached and then the saturation state merely indicates in which direction the processes may occur. In case of undersaturation, dissolution is expected, while oversaturation suggests mineral precipitations (Appelo and Postma 1994). These indices of saturation show that water is saturated to

oversaturated with respect to carbonates minerals (calcite, aragonite and dolomite), saturated with respect to gypsum and anhydrite and undersaturated with respect to halite (Fig. 8).

Most of the water sampled is saturated with respect to calcite (SI < 1, Fig. 7c). Calcite precipitation may occur systematically for all groundwater samples (Fig. 8a).

For all groundwater samples, there is an equilibrium state with gypsum (1 < SI < –1) which confirms the role of gypsum dissolution (Fig. 8d).

Isotopic study

Stable isotopes

Interpretation of oxygen-18 and deuterium data

Stable isotopes of water molecule are indicators of conditions at the time and place of groundwater recharge (Faure 1986). They are influenced by phase change processes affecting the water and can help to identify waters

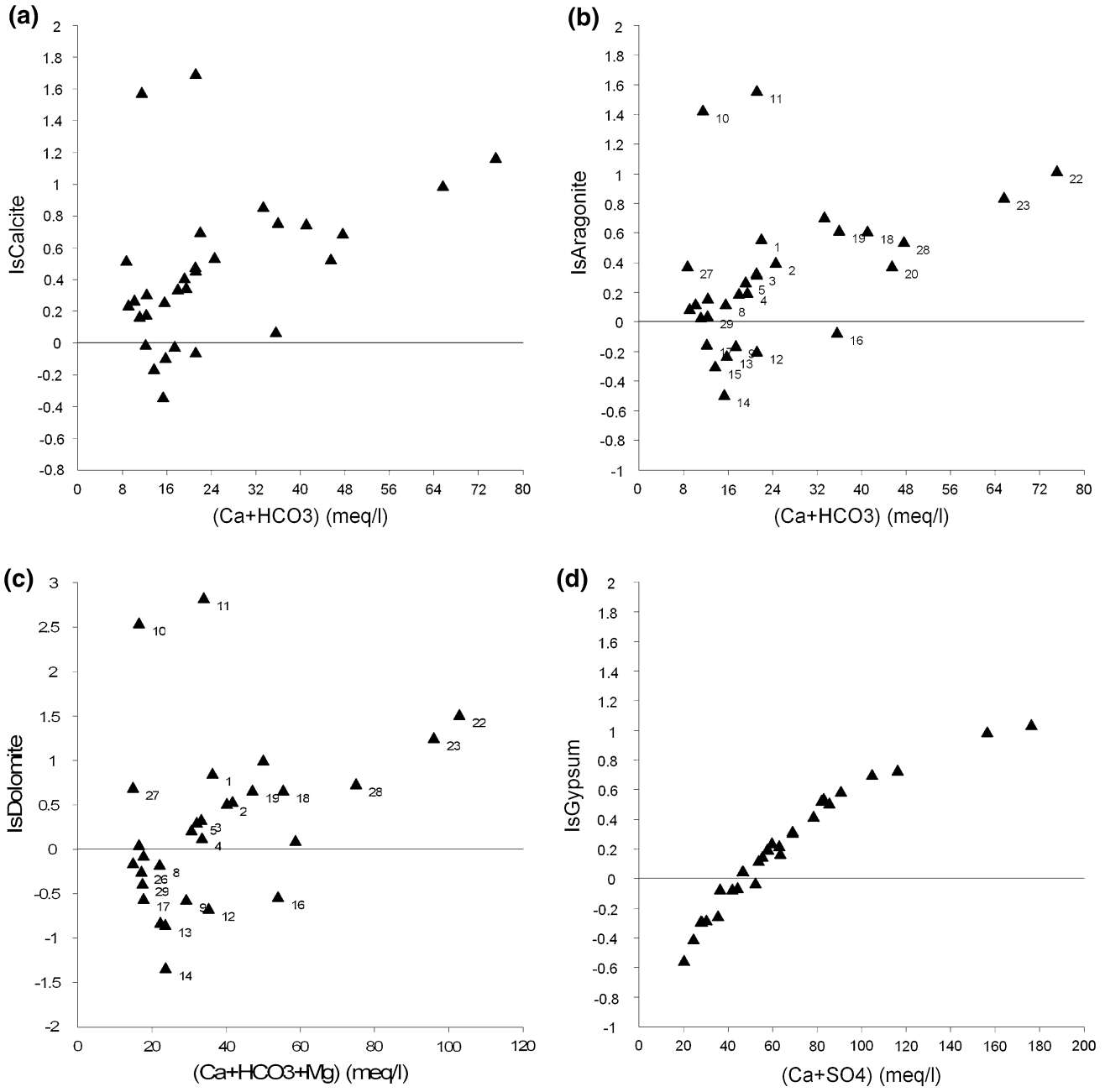

Fig. 8 Saturation indices of calcite (**a**) and aragonite (**b**) versus (Ca^{2+} + HCO_3^-), of dolomite (**c**) versus (Ca^{2+} + HCO_3^- + Mg^{2+}), of gypsum (**d**) and anhydrite (**e**) versus (Ca^{2+} + SO_4^{2-}), and of halite (**f**) versus (Na^+ + Cl^-)

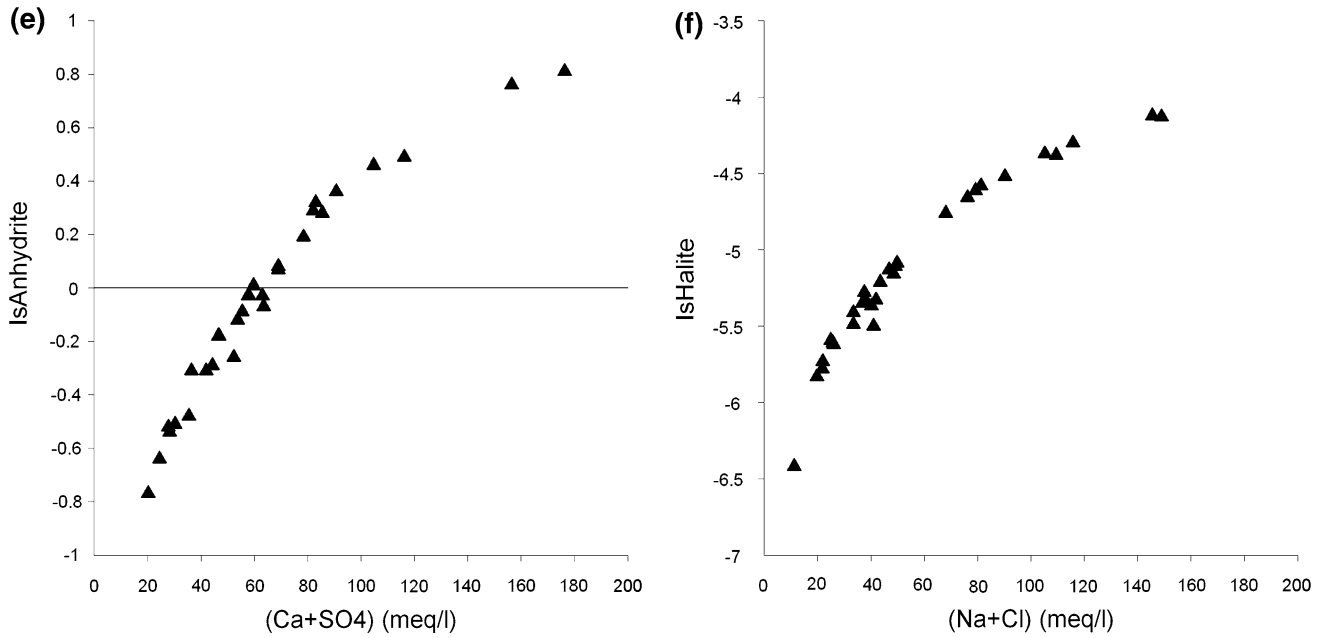

Fig. 8 continued

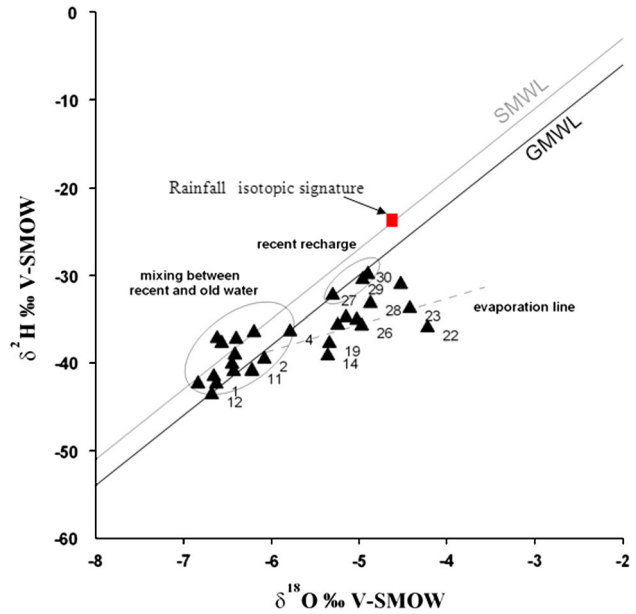

Fig. 9 δ^2H–$\delta^{18}O$ relationship for the intermediate aquifer of the Sfax basin

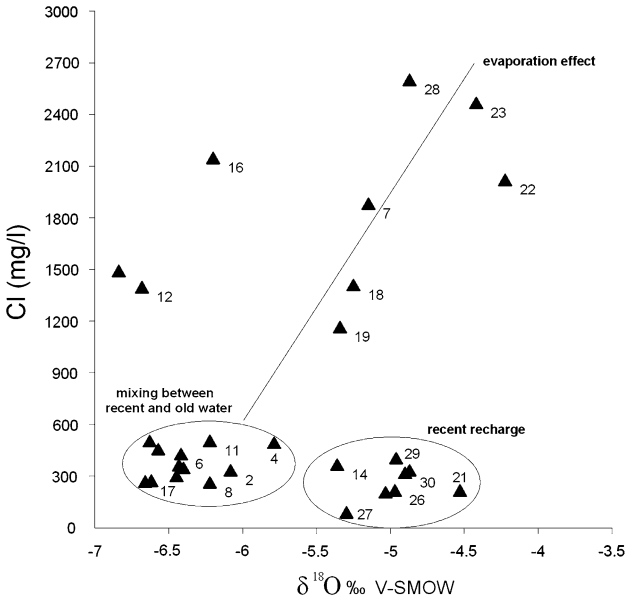

Fig. 10 $\delta^{18}O$–Cl relationship for the intermediate aquifer groundwaters

that have undergone evaporation and recharge under different climatic conditions. They can also help to resolve overall questions relating to mixing of waters from different sources (Sacks and Tihansky 1996). The δ^2H and $\delta^{18}O$ signatures of groundwater are generally compared to those of the precipitation represented by the global meteoric water line (GMWL) (Craig 1961) and the regional meteoric water line (RMWL). Considering only the highest rainfall events (>5 mm), the regional meteoric water line (RMWL) is obtained for Sfax in thermodynamic equilibrium conditions (slope of 8) is: $\delta^2H = 8$ δ18O + 13.5.

The relatively high value of the deuterium excess (d), 13.5, reflects the participation of condensing vapour of Mediterranean air masses (Maliki 2000). Results from the studied aquifer are shown in Fig. 9 in relation to the global meteoric water line (GMWL) and the Sfax meteoric water line (RMWL).

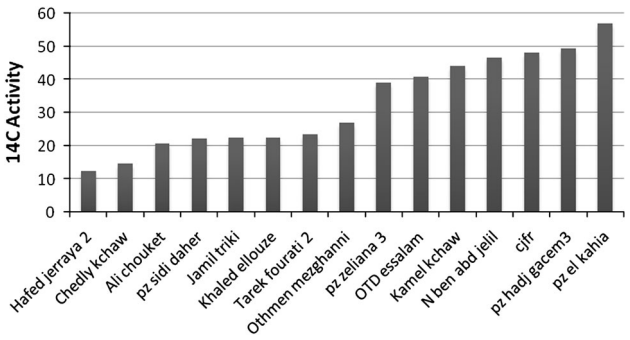

Fig. 11 ^{14}C Activity of groundwater of the intermediate aquifer

The measured stable isotope composition of the studied aquifer is quite variable; $\delta^{18}O$ ranges from −4.2 to −5.3 % with corresponding $\delta^{2}H$ values ranging from −29.9 to −36 %.

The $\delta^{18}O/\delta^{2}H$ diagram (Fig. 9) shows that the sampled groundwater lies as a group on or below the meteoric water lines. The composition of water in the intermediate aquifer collected close to the Mio–Plio–Quaternary outcrops (samples 27, 29, 30) lies on the GMWL and has averages values of $\delta^{18}O = -5$ ‰, $\delta^{2}H = -30.9$ ‰. This group shows the same isotopic signature as that of precipitation (the average values of rainfall events higher than 5 mm are $\delta^{18}O = -4.6$ and $\delta^{2}H = -23.3$ ‰ V-SMOW: Moncef Zaïri, Boubaker El-Euch; Plummer et al. 1976).These non-evaporated groundwaters with relatively enriched contents, reflecting recharge at lower altitudes, highlight the influence of return flow of irrigation waters. This result indicates the likelihood of recent rainwater infiltration without any evaporation effect.

Some other points located at the vicinity of the meteoric water lines (δ18O ranges from −5.79 to −6.8 %) show a higher depletion than in recent precipitation. This group may represent a mixing between old and recent water. This is confirmed by the high nitrate contents (82.05 mg/l in well (Tarek Fourati) and 89.15 mg/l in well (Zied Fourati). The waters found below the first group also indicate that the climate was different from that of present day with a cooler regime.

A third group shows a wide scatter and a wide range of ^{18}O enrichment (evolution below the meteoric water line). Most of these waters are strongly evaporated as shown by their positions below the GMWL and the SMWL. This suggests that they were infiltrated through stagnating parts of the Sebkhas (Sebkha Mechguigue, Sebkha Bou Jmal and Sebkha En Noual), which made stronger evaporation possible. The intersection of this evaporation line with the GMWL gives values of −6 and −40 ‰ for the respective $\delta^{18}O$ and $\delta^{2}H$ content of the recharging precipitation before evaporation.

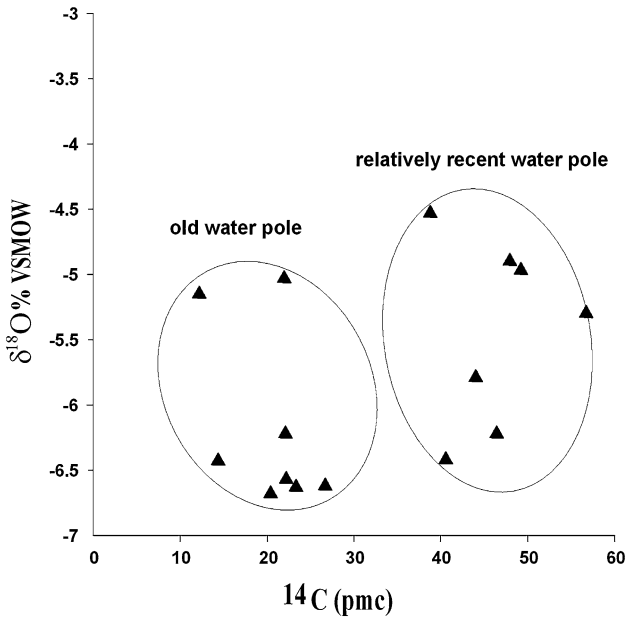

Fig. 12 Plot of $\delta^{18}O$ versus ^{14}C (pmc) of intermediate aquifer

Chloride versus $\delta^{18}O$

The chloride content is plotted against oxygen isotope composition in Fig. 10, to discriminate more precisely the different waters involved in the mixing, recent rainwater infiltration and the evaporation effect, which affect some samples of this aquifer.

In this diagram, the first trend indicating the mixing between old and recent waters includes isotopically depleted waters (−5.8 to −6.7 ‰) with low chloride concentrations (<600 mg/l).

The dilute groundwaters are found at shallow depths (80–175 m). These waters have a mean Cl^{-} concentration of about 300 mg/l and are enriched in $\delta^{18}O$ with a mean value of about −5 ‰. This strongly suggests that these groundwaters are influenced directly by the infiltration of local precipitation.

The third trend shows that little evaporation occurs during infiltration of the local precipitation. Samples constituting this trend show systematic increase in $\delta^{18}O$ and chloride by evaporation effect.

The importance of dissolution of evaporites (halite, anhydrite and/or gypsum) and evaporation process are observed in the Cl vs $\delta^{18}O$ diagram (Fig. 10), which includes data for groundwater collected in this study. It is noted for the major part of groundwater samples that high chloride concentrations are not clearly correlated with the oxygen-18 contents. This heterogeneous arrangement is mainly due to the dissolution of evaporite deposits.

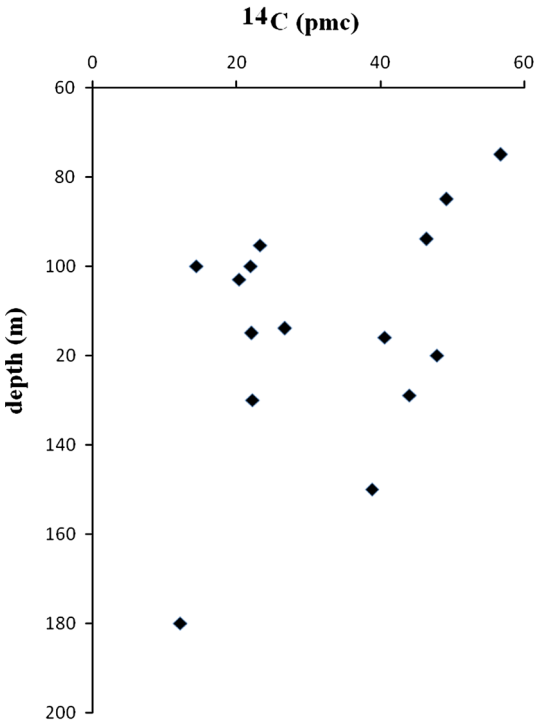

Fig. 13 ^{14}C Activity vs depth in the intermediate aquifer (data are reported in Table 1)

Carbon isotopes content and groundwater age dating

Isotopic methods of groundwater dating have made it possible to estimate the mean ages of groundwater pumped from wells (Bethke and Johnson 2008; Kazemi et al. 2008). Carbon-14 is a widely used radiometric dating technique for groundwater because of the almost ubiquitous presence of dissolved inorganic carbon (DIC). This technique exploits the decay of ^{14}C from the onset of recharge to estimate groundwater age at locations along the flowpath.

The ^{14}C dating method is not without problems, though many of them have been addressed to minimize uncertainties (Mokrik et al. 2008; Coetsiers and Walraevens 2009; Cartwright 2010). In principle, combining groundwater age dates with isotopic characterization and interpretation of chemical composition provides important information on the timing, rate and sources of recharge (Maduabuchi et al. 2006), which in most cases guide assessment of groundwater sustainability.

Groundwaters sampled from the intermediate aquifer (80–200 m in depth) have $^{14}CDIC$ values between 12.2 and 56.7 pmc (Table 1, Fig. 11). The relatively high activities give evidence of the existence of a large fraction of organic ^{14}C, likely in relation with the infiltration of rain waters, which affects the initial ^{14}C contents. However, the low activities of ^{14}C indicate the ancient origin of the intermediate groundwaters in the study area.

The relationship between measured ^{14}C values and $\delta^{18}O$ (Fig. 12) shows two types of water groups, in agreement with the results obtained from the hydrochemistry and stable isotopes analyses. As shown in Fig. 11, the dilute groundwaters are found at shallow depths, in communication with the Plio–Quaternary aquifer. These waters have a mean ^{14}C content of 46.8 pmc and mean $\delta^{18}O$ value of about −5.3 ‰. Old waters have lower mean ^{14}C values (19.4 pcm) and more depleted ^{18}O content (−6 ‰) in keeping with their long residence time in the aquifer. This is confirmed by the variation of ^{14}C with depth as shown in Fig. 13. Indeed, the lowest ^{14}C content (12.2) is found in the Hafed Jerraya well at a depth of 180 m, whereas the highest ^{14}C value (56 pcm) is attributed to the piezometer El kahia at a depth of 75 m.

Conclusion

The combination of both hydrochemical and isotopic investigations of groundwater in the aquifer of Sfax basin has helped to better characterize the main features of salinization of local groundwaters in this sector. Chemical analysis showed that the groundwaters are generally of two types of systems: sodium chloride and sodium sulphate.

Closer analysis of available chemical data reveals the importance of dissolution/precipitation processes as well as cations exchange reactions in the evolution of groundwater chemistry. In general, mineralization of groundwater increases along the flow path from the N–S mountain axis in the north to the Mediterranean Sea in the south. The Na^+/Cl^-molar ratio suggests that the dissolution of halite in evaporites within the Mio–Plio–Quaternary sequences are the main sources of these ions in groundwater. The values of this ratio, higher than 1, observed in the majority of the groundwater samples may indicate the occurrence of cation exchange reactions releasing Na^+ into the water with simultaneous removal of Ca^{2+}. The existence of such exchange is confirmed by the balance between the excess of $(Na^+ + K^+)$ over the Cl^-ions and excess of $(Ca^{2+} + Mg^{2+})$ over the $(HCO_3^- + SO_4^{2-})$ anions. The exchange phenomenon and basic processes of dissolution/precipitation of carbonate minerals (calcite and dolomite) are usually the cause of the wide variation in concentrations of cations (Ca^{2+}, Mg^{2+} and Na^+) in groundwater.

Chemical data also indicate the importance of gypsum dissolution as a factor controlling groundwater chemistry. The occurrence of low-saline waters at the N–E and in the western part of the study area suggests local recharge of this intermediate aquifer by the shallow aquifer through faults and/or semi-permeable layers.

The isotopic study provided a better understanding of the hydrodynamic functioning of the studied aquifer and

the origin of the groundwater mineralization. Based on stable isotopes, the N–S axis mountain chain to the west and the Korj Bou Thadi, Chorbanehills to the north are considered as the main areas of groundwater recharge.

The stable isotope composition of waters permits the distinction between three groups of groundwater samples:

1. The first group shows the same isotopic signature as the rainfall events higher than 5 mm, which indicates the presence of a young local component not affected by any evaporation.
2. The second group is characterized by a greater isotopic depletion relative to recent precipitations. This group represents the most depleted isotopic signature of this intermediate aquifer of the Sfax basin.
3. The third group is represented by the most isotopically enriched groundwater samples.The majority of the points representing this group are strongly evaporated as shown by their positions below the GMWL and the SMWL.

The relationship between oxygen-18 and chloride content suggests the existence of different processes at the origin of water salinity variation. The deepest water of the studied aquifer showed the most depleted values of stable isotopes and low activities of ^{14}C.

Obviously, continued water utilization in the coastal and near-coastal areas would further increase the depletion of water resource and degradation of groundwater quality. These factors should take into consideration in future water management plans: decrease pumping from the more vulnerable and contaminated coastal groundwater and further exploration of the high-quality and renewable water resources in the upper zone of the Sfax basin. Moreover, the results of this study indicate that future exploration of the intermediate groundwater from the Mio–Plio–Quaternary semi-confined aquifer would result in production of good-quality water but with old ages in some regions, which is inferred as exploitation of non-renewable water resource.

References

Abid K, Trabelsi R, Zouari K, Abidi B (2009) Caractérisation hydrogéochimique de la nappe du Continental Intercalaire (Sud tunisien) [Hydrogeochemical characterization of the Continental Intercalaire aquifer (southern Tunisia)]. J Sci Hydrol 54(3):526–537

Abid K, Zouari K, Dulinski M, Chkir N, Abidi B (2010) Hydrologic and geologic factors controlling groundwater geochemistry in the Turonian aquifer (southern Tunisia)

Appelo CAJ, Postma D (1994) Geochemistry, groundwater and pollution, 2nd edn. A.A. Balkema, Rotterdam

Aravena R, Wassenaar LI, Plummer LN (1995) Estimating 14C groundwater ages in a methanogenic aquifer. Water Resour Res 31(9):2307–2317

Belgacem A, Kharroubi A, Bouri S, Abida H (2010) Contribution of geostatistical modelling to mapping groundwater level and aquifer geometry, case study of Sfax's deep aquifer. Tunis Middle East J Sci Res 6(3):305–316

Ben Akacha M (2001) Etude géologique de la région d'Agareb-Sfax : évolution géomor-phologique néotectonique et paléogéographique. DEA, Faculté des Sciences de Sfax, p 94

Beni Akhy R (1994) Evolution et modélisation de la nappe phréatique urbaine de Sfax. Mémoire de DEA, Faculté des Sciences de Tunis

Bennetts DA, Webb JA, Stone DJM, Hill DM (2006) Understanding the salinisation process for groundwater in an area of south-eastern Australia, using hydrochemical and isotopic evidence. J Hydrol 323:178–192

Bethke CM, Johnson TM (2008) Groundwater age and groundwater age dating. Annu Rev Earth Planet Sci 36:121–152

Bouaziz S (1994) Eude de la tectonique cassante dans la plate-forme et l'Atlas Saharien (Tunisie méridionale) : évolution des paléo-champs de contraintes et implication géodyna-mique. Thèse. Doc. Etat. Sc. Geol. Univ. Tunis II. p 485

Burollet (1956) Contribution à l'étude Stratigraphique de la Tunisie Centrale, Annale des mines et de la Géologie 18:345

Cartwright I (2010) Using groundwater geochemistry and environmental isotopes to assess the correction of 14C ages in a silicate-dominated aquifer system. J Hydrol 382(1–4):174–187

Castany G (1953) Les plissements quaternaires en Tunisie. Comptes Rendus Sommaires Société Géologique de France, Paris, pp 155–157

Clark I, Fritz P (1997) Environmental isotopes in hydrogeology. Lewis Publishers, Boca Raton

Coetsiers M, Walraevens K (2009) A new correction model for 14C ages in aquifers with complex geochemistry–application to the Neogene Aquifer, Belgium. Appl Geochem 24(5):768–776

Craig H (1961) Isotopic variation in meteoric waters. Science 133:1702–1703

Custodio E (1987) Hydrogeochemistry and tracers. In: Custodio E (ed), Groundwater problems in coastal areas. Studies and reports in hydrology, vol 45. UNESCO, Paris, pp 213–269

Dansgaard W (1964) Stable isotopes in precipitation. Tellus 16:436–438

Dixon W, Chiswell B (1992) The use of hydrochemical sections to identify recharge areas and saline intrusions in alluvial aquifers, southeast Queensland, Australia. J Hydrol 130:299–338

Edmunds WM, Guendouz AH, Mamou A, Moulla A, Shand P, Zouari K (2003) Groundwater evolution in the Continental Intercalaire Aquifer of southern Algeria and Tunisia; trace element and isotopic indicators. Appl Geochem 18:805–822

El Batti and Andrieux (1977) Etude hydrogéologique et géophysique du secteur Wadrane. Rapport interne

Faure G (1986) Principles of isotope geology. Wiley, New York

Fedrigoni L, Krimissa M, Zouari K, Maliki A, Zuppi GM (2001) Origine de la minéralisation et comportement hydrogéochimique d'une nappe phréatique soumise à des contraintes naturelles et anthropiques sévères: exemple de la nappe de Djebeniana (Tunisie). Earth Planet Sci Lett 332:665–671

Fontes J-C, Garnier J-M (1979) Determination of the initial 14C activity of the total dissolved carbon: a review of the existing models and a new approach. Water Resour Res 15(2):399–413

Garcia MG, Del Hidalgo M, Blesa MA (2001) Geochemistry of groundwater in the alluvial plain of Tucumán province Argentina. Hydrogeol J 9(6):597–610

Guendouz A, Moulla AS, Edmunds WM, Zouari K, Shand P, Mamou A (2003) Hydrogeochemical and isotopic evolution of water in the complex terminal aquifer in the Algerian Sahara. Hydrogeol J 11:483–495

Hajjem A (1980) Etude hydrogéologique de la région de Sidi Abid. Rapport interne, vol 8. DRES, Tunis

Kazemi AG, Lehr JH, Perrochet P (2008) Groundwater age. Wiley-Interscience, New York

Maduabuchi C, Faye S, Maloszewski P (2006) Isotope evidence of palaeorecharge and palaeoclimate in the deep confined aquifers of the Chad Basin, NE Nigeria. Sci Total Environ 370:467–479

Magaritz M, Nadler A, Koyumdjisky H, Dan N (1981) The use of Na/Cl ratio to trace solute sources in a semiarid zone. Water Resour Res 17:602–608

Maliki A (2000) Etude hydrogéologique, hydrochimique et isotopique de la nappe profonde de Sfax (Tunisie), thèse, ENIS

Maliki A, Krimissa M, Michelot JL, Zouari K (2000) Relation entre nappes superficielles et aquifère profond dans le bassin de Sfax (Tunisie). Earth Planet Sci 331:1–6

McLean W, Jankowski J, Lavitt N et al (2000) Groundwater quality and sustainability in an alluvial aquifer, Australia. In: Sililo O (ed) Groundwater, past achievement and future challenges. Balkema, Rotterdam, pp 567–573

Mokrik R, Mazeika J, Baublyte A, Martma T (2008) The groundwater age in the Middle–Upper Devonian aquifer system, Lithuania. Hydrogeol J 17(4):871–889

Petalas CP, Diamantis IB (1999) Origin and distribution of saline groundwaters in the upper Miocene aquifer system, coastal Rhodope area, northeastern Greece. Hydrogeol J 7:305–316

Petalas C, Pisinaras V, Gemitzi A, Tsihrintzis VA, Ouzounis K (2009) Current conditions of saltwater intrusion in the coastal Rhodope aquifer system, northeastern Greece. Desalination 237:22–41

Piper AM (1944) A graphic procedure in the geochemical interpretation of water analyses. EOS Trans Am Geophys Union 25:914–923

Plummer LN, Jones BF, Truesdell AH (1976) WATEQF, a Fortan IV version of WATEQ, a computer program for calculating chemical equilibrium of natural waters. US Geol Surv Water Resources Invest 76:61

Rahoui H, Koshel R (1980) Cartes des ressources en eau souterraine de la Tunisie à l'échelle du 1:200000. Feuille de Sbeïtla No. 14. Divisions des ressources en eau

Richter BC, Kreitler CW (1993) Geochemical techniques for identifying sources of ground-water salinization. CRC Press, Boca Raton

Rozanski K, Araguas–Araguas L, Gonfiantini R (1993) Isotopic patters in modern global precipitation. In: Swart PK et al (eds) Climate change in continental isotopic records. Geophysical Monograph Series, vol 78. AGU, Washington, pp 1–36

Sacks LA, Tihansky AB (1996) Geochemical and isotopic composition of ground water, with emphasis on sources of sulfate, in the upper Floridan aquifer and intermediate aquifer system in Southwest Florida. Water-resources investigations reports, US Geol Surv, pp 96–4146

Tayech B (1984) Etudes palynologiques dans le Néogène du Cap Bon (Tunisie). Thèse de Doct. 3ème cycle. Unv. Claude Bernard, Lyon I

Trabelsi R, Zaïri M, Smida H, Ben Dhia H (2005) Salinisation des nappes côtières: cas de la nappe nord du Sahel de Sfax, Tunisie. C. R. Acad. Sci. Paris 337:515–524

Trabelsi R, Kacem A, Zouari K, Rozanski K (2008) Quantifying regional groundwater flow between continental Intercalaire and Djeffara aquifers in southern Tunisia using isotope methods. Environ Geol 58:171–183

Vengosh A (2003) Salinization and saline environments. In: Sherwood Lollar B (ed), Environmental geochemistry, Treatise in Geochemistry, vol 9. Elsevier Science, New York

Vengosh A, Gert J, De Lange GJ, Starinsky A (1998) Boron isotope and geochemical evidence for the origin of Urania and Bannock brines at the eastern Mediterranean: effect of water–rock interactions. Geochim Cosmochim Acta 62:3221–3228

Vengosh A, Kloppmann W, Marie A, Livshitz Y, Gutierrez A, Banna M, Guerrot C, Pankratov I, Ranan H (2005) Sources of salinity and boron in the Gaza Strip: natural contaminant flow in the southern Mediterranean Coastal aquifer. Water Resour Res 41:W01013. doi:10.1029/2004WR003344

Vengosh A, Hening S, Ganor J, Mayer B, Weyhenmeyer CE, Bullen TD, Paytan A (2007) New isotopic evidence for the origin of groundwater from the Nubian Sandstone Aquifer in the Negev, Israel. Appl Geochem 22:1052–1073

Zébidi H (1989) Hydrogéologie de la nappe profonde de Sfax. Rapport D.G.R.E. Tunis, p 27